

Cite this: *RSC Sustainability*, 2025, 3, 5176

Visible-light-induced decarboxylative acylation of unsaturated hydrocarbons with α -oxocarboxylic acid via Csp^2-Csp^2 cross-coupling: a facile access to chalcones

Aman Singh,^{†a} Ambuj Kumar Kushwaha,^{†b} Shikha Pandey,^a Pooja Kumari,^a Ankur Yadav^a and Sundaram Singh^{id} *^a

We describe a streamlined and efficient strategy for synthesizing chalcones *via* photocatalytic decarboxylative cross-acyl coupling of α -oxocarboxylic acid with styrene, employing an organic photoredox catalyst under visible light irradiation as a sustainable energy input. Detailed mechanistic studies demonstrate that the transformation proceeds through a radical mechanism. Furthermore, the broad functional group tolerance, compatibility with structurally complex and biorelevant substrates, and facile scalability collectively underscore the robustness and synthetic utility of the developed methodology. This methodology holds significant promise for the late-stage modification of bioactive molecules and natural products.

Received 19th August 2025
Accepted 25th September 2025

DOI: 10.1039/d5su00684h

rsc.li/rscsus

Sustainability spotlight

This study presents a novel method that follows the principles of green chemistry, highlighting sustainability and low energy costs. Many researchers are interested in possible applications of visible light as an energy source in organic synthesis since it is a particularly sustainable source of energy. Our ongoing interest is in metal-free photoredox processes; thus, we have developed an efficient, straightforward, and sustainable approach for C–C bond synthesis through the decarboxylative hydroacylation of aryl alkenes with α -oxocarboxylic acids without using any metal catalyst. This approach exhibits good compatibility with functional groups, including hetero(aryl) alkenes, and a wide range of substrates. Finally, this process shows potential for the synthesised chalcone analogues with therapeutic applications. Greener catalytic and solvent systems, as well as extending the substrate broadness to include more α -oxocarboxylic acid and styrene derivatives, will be the primary objectives of future work.

Introduction

The unprecedented reactivity of photoredox catalysis through radical interactions has revitalized traditional transition metal catalysis and cross-coupling reactions, leading to extensive research in photocatalytic C–C bond formations for synthetic chemistry.^{1,2} Carboxylic acids are a vital class of chemicals widely used in various industries, appreciated for their high stability, low toxicity, and easy accessibility.³ The decarboxylative coupling of carboxylic acids has garnered significant attention from organic chemists, emerging as one of the most efficient strategies for the construction of C–C and C–X (X = N, P, S) bonds.^{4,5} This area of research has extensively investigated a diverse array of carboxylic acids, encompassing aromatic, aliphatic, α,β -unsaturated, and α -oxocarboxylic acids.⁶

α -Oxocarboxylic acids are widely utilized as efficient agents for the insertion of carbonyl groups into organic compounds (Scheme 1a).⁷ Photocatalyzed decarboxylative cross-coupling processes using α -oxocarboxylic acids as acylating agents have demonstrated remarkable selectivity and broad functional group tolerance, enabling the efficient synthesis of aryl ketones.⁸ The potential for using stable and easily accessible α -oxocarboxylic acid with CO₂ as the only waste product has garnered significant interest in photocatalyzed decarboxylative cross-coupling processes.⁹ With the benefits of atom economy, mild operating conditions, and broad substrate tolerance, this greener process offers an efficient route to chalcone derivatives through the hydroacylation of alkenes, which remains underdeveloped. Chalcone drugs exhibit a broad spectrum of pharmacological activities, including anti-inflammatory, anti-tumour, antioxidant, anti-tuberculosis, and anti-diabetic effects.^{10–13} In light of the medicinal importance of chalcones, some synthetic approaches have been developed by organic chemists in recent years (Scheme 1b).

In 2015, Can-Cheng Guo *et al.* reported an iron-mediated decarboxylative cross-coupling of α -oxocarboxylic acids with acrylic acid (Scheme 1b-ii).¹⁴ Subsequent transition metal-

^aDepartment of Chemistry, Indian Institute of Technology (BHU), Varanasi-221 005, U.P., India. E-mail: sundaram.apc@iitbhu.ac.in; Tel: +919451658650

^bDepartment of Chemistry, Janta Vedic College, Baraut, Baghpat-250611, India

[†] These authors contributed equally to this paper.





Scheme 1 Latest strategies for decarboxylation of α -oxocarboxylic acids. (a) Decarboxylation of α -oxocarboxylic acids, (b) access to chalcones via decarboxylation of α -oxocarboxylic acids, (c) our work-access to chalcones via metal-free decarboxylation.

catalyzed methods have expanded its utility, particularly in the synthesis of chalcones. Utilizing silver as a catalyst, Shang Wu *et al.* developed a decarboxylative coupling of α -oxocarboxylic acids with alkenes (Scheme 1b-i).¹⁵ Due to the high cost and limited availability of metal catalysts, alternative pathways for chalcone synthesis have been explored. In 2017, the Chengjian Zhu group introduced a photocatalyzed decarboxylative cross-coupling of α -oxocarboxylic acids with styrene, using an iridium catalyst, and in 2022 the Tunge group synthesized chalcones using a cobalt catalyst (Scheme 1b-iii)^{16,17}

More recently, Pradyut Ghosh *et al.* reported a double decarboxylation and Pd-photocatalyzed method for Csp²-Csp² coupling (Scheme 1b-iv).¹⁸ From a green chemistry perspective, replacing expensive precious metal catalysts or photocatalysts with cost-effective organic dyes offers an ideal solution to address future resource limitations. In line with our ongoing interest in visible light mediated reactions,^{19–26} herein, we have developed a green, effective, facile, and metal-free method for C-C bond synthesis via decarboxylative hydroacylation of aryl alkenes with α -oxocarboxylic acids (Scheme 1c).

Results and discussion

At the outset of our study on decarboxylative coupling, we chose α -oxocarboxylic acid (1a) as the model acyl radical precursor

Table 1 Optimization of reaction conditions^a

Entry	Deviation from the model reaction	Yield ^b (%)
1	None ^a	32
2	Different photocatalysts	Trace
3	Different bases instead of NaHCO ₃	10–25
4	CH ₃ CN instead of ethanol	48
5	H ₂ O instead of ethanol	42
6	Methanol instead of ethanol	25
7	Non-polar solvents	11–16
8	Different ratios of MeCN : H ₂ O	64–88
9	1, 2, and 4 mol% of eosin Y	70–79
10	14, 16, and 20 h instead of 18 h	75–87
11	Different LEDs instead of blue LED	54–71
12	Without PC	nr
13	In the dark	nr

^a Reaction conditions: α -oxocarboxylic acid (0.25 mmol), styrene (0.25 mmol), eosin Y (3 mol%), MeCN and water (5 mL), in visible light (18 h) under open air at room temperature. ^b Isolated yield.





Scheme 2 Substrate scope of α -oxocarboxylic acid and styrene. ^aReaction conditions: α -oxocarboxylic acid (0.25 mmol), styrene (0.25 mmol), eosin Y (3 mol%), MeCN and water (5 mL), in visible light (18 h) under open air at room temperature. ^bIsolated yield.

and styrene (**2a**) as the representative alkene partner under blue light irradiation ($\lambda_{\text{max}} = 455 \text{ nm}$) at room temperature (Table 1).

At the outset of our study on decarboxylative coupling, we chose α -oxocarboxylic acid (**1a**) as the model acyl radical precursor and styrene (**2a**) as the representative alkene partner under blue light irradiation ($\lambda_{\text{max}} = 455 \text{ nm}$) at room temperature (Table 1). After screening several photocatalysts (Table 1, entry 2), eosin Y was determined to have the highest yield (32%). A range of bases was examined, and it was found that 2 equiv. of NaHCO₃ had the best reaction efficiency (Table 1, entry 3). After that, different polar and nonpolar solvents were optimized and found that polar solvents gave better yields (15–48%) in comparison to nonpolar solvents (11% and 16%) (Table 1,

entries 4–7). Guided by ongoing research in our lab and previous reports, we tested with various proportions of MeCN to H₂O (Table 1, entry 8). Our optimization revealed that a 2 : 1 ratio was ideal, boosting the yield to 88%. The product yield decreased when the photocatalyst's mole percentage was either increased or decreased (Table 1, entry 9). A comparable yield was obtained when the reaction time was extended (Table 1, entry 10). The reaction yield was lowered when we used alternate coloured LEDs, indicating the strong influence of the blue LEDs (Table 1, entry 11). Additionally, no product was obtained in the absence of the photocatalyst or in the dark, demonstrating the necessity for the photocatalyst and light (Table 1, entries 12 and 13). Based on the above testing, the optimal





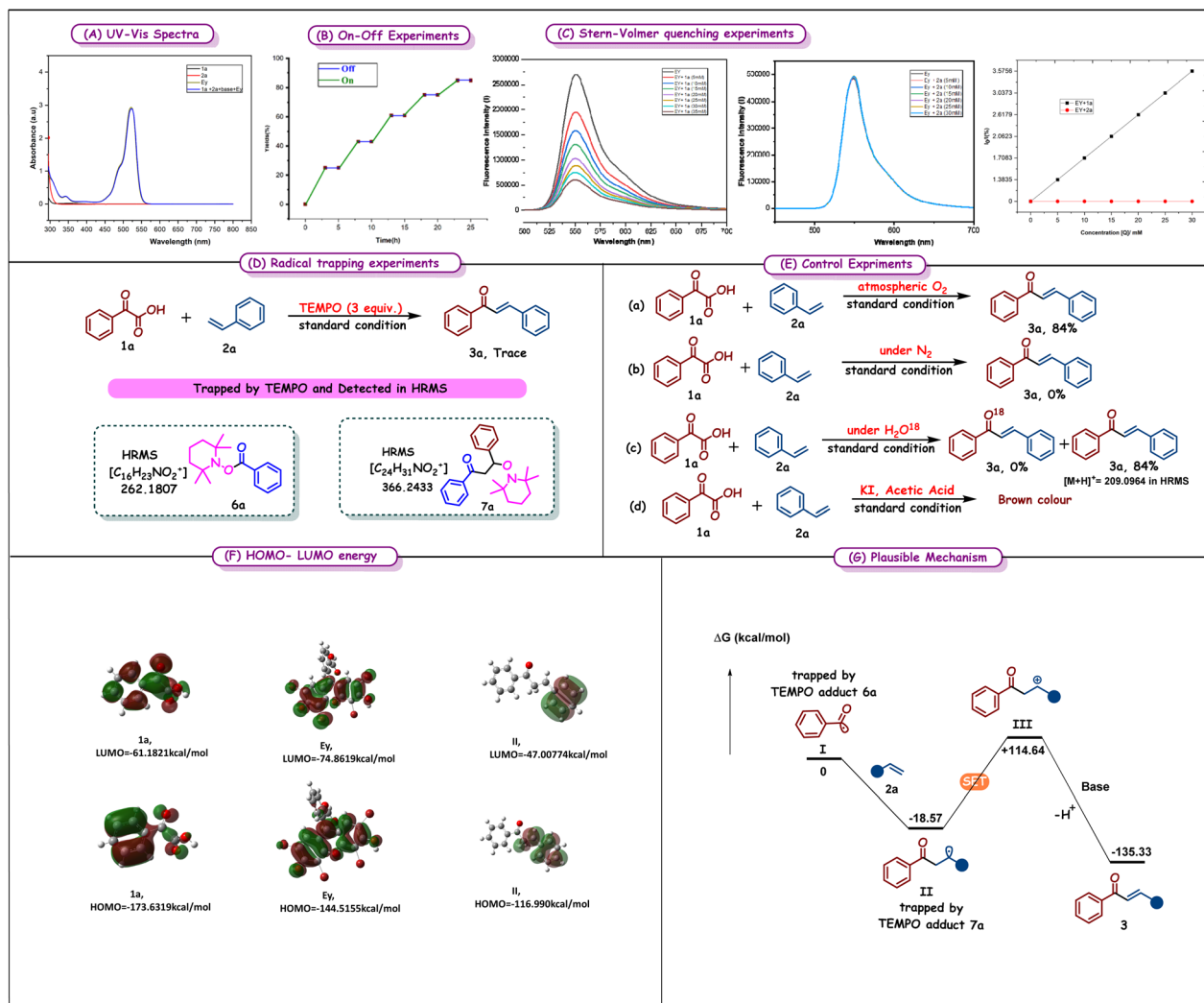
Scheme 3 Gram-scale synthesis of product 3a.

conditions were achieved with 3 mol% eosin Y in MeCN : H₂O (2 : 1, 5 mL) under blue light irradiation for 18 hours.

After getting the optimized reaction conditions, the scope for photoinduced acylation of styrene was explored. Using α -oxocarboxylic acid (1a) as a substrate, a wide variety of structurally and electronically distinct styrenes were afforded (Scheme 2a). Investigations into functional groups, such as electron-withdrawing groups like nitro and halo and electron-donating groups like methoxy and methyl, were well tolerated and yielded the intended product in 59–88% yields (3b–3f). Furthermore, the yield of the substrates with *ortho*- and *meta*-position substituents (3g–3i) on styrene was significantly lower, 56–78%,

compared to that of the substrates with *para*-position substituents. This revealed that substrates with substituents in the *meta*-position rather than the *para*-position showed modest reactivity, and there was a noticeable steric effect. The coupling with more sterically hindered, disubstituted, and trisubstituted styrene rings was also studied, and a moderate to good yield of the intended products was obtained (3j–3m). We prepared a diverse set of chalcones using heterocyclic styrenes like 2-vinylfuran, 2-vinylthiophene, and 2-vinylpyridine (3n–3p) and polyaromatic styrenes like 1-vinylnaphthalene and 9-vinylanthracene (3q–3r) in 73–78% yields.

Furthermore, we investigated the effect of substitution at the *para*-position of α -oxocarboxylic acid (1a) and observed that the substrates with electron-donating (Scheme 2c, 5e–5g, 5i, 5j) and electron-neutral (Scheme 2a) groups exhibited slightly greater reactivity than those with electron-withdrawing substitutions (Scheme 2b, 4a–4n). The generality of our hypothesis for bioactive molecules was demonstrated by synthesizing compound 5b, which showed antistaphylococcal activity, and



Scheme 4 Mechanistic studies and plausible mechanism. (A) UV-visible spectra. (B) Light ON–OFF experiment. (C) Stern–Volmer quenching experiment. (D) Radical trapping experiment with TEMPO. (E) Control experiments. (F) HOMO–LUMO energy levels. (G) Plausible mechanism.



compounds **5a**, **5c–5d** showing antibacterial activities.^{27,28} Furthermore, when the reaction was carried out on a 5.0 mmol scale, there was minimal variation in the yield of product **4a**, indicating that this methodology was compatible with the gram scale (Scheme 3). To gain a deeper understanding of the decarboxylative coupling reaction mechanism, we conducted several control experiments. We performed UV-visible spectroscopy of the reactants, reaction mixture, and eosin Y (Scheme 4A). The outcomes showed that while the reaction mixture and eosin Y both showed absorbance in the visible range, the reactants showed no absorbance in that area. To show the interaction between excited eosin Y and reactants, we carried out several fluorescence quenching tests, demonstrating that **1a** could efficiently quench excited eosin Y. A direct interaction between excited eosin Y and **1a** was indicated by a linear relationship on the Stern–Volmer plot. A straight line parallel to the *X*-axis on the Stern–Volmer plot rules out the possibility of a direct interaction between excited eosin Y and **2a** (Scheme 4C). We conducted a light ON/OFF experiment, which revealed that continuous light irradiation was necessary for product formation (Scheme 4B). A lower yield of the desired product **3a** was observed when the model reaction was performed in the presence of TEMPO (a radical scavenger) (Scheme 4D). High-resolution mass spectrometry (HRMS) analysis revealed the formation of TEMPO adducts **6a** and **7a**. This finding supports our point that the reaction goes through a radical pathway. We conducted additional control experiments (Scheme 4E), and when the reaction was carried out under an external oxygen atmosphere, no significant change in yield was observed (Scheme 4E-a). This suggests that the reaction proceeds efficiently under ambient atmospheric oxygen. No product formation was observed when the reaction was conducted under a nitrogen atmosphere, highlighting the crucial role of oxygen in facilitating the transformation (Scheme 4E-b). In order to clearly identify whether the oxygen atom responsible for toluene oxidation is derived from atmospheric oxygen or water, an isotope-labeling study was performed using H₂O.¹⁸ The absence of any labeled product (Scheme 4E-c) indicates that water does not contribute the oxygen atom in this transformation. To investigate the formation of H₂O₂, the reaction mixture was added to a freshly prepared solution of KI and acetic acid. A brown coloration was observed, indicating the liberation of iodine. This result confirms the presence of H₂O₂ in the system, suggesting the involvement of superoxide radical anion species in the reaction pathway (Scheme 4E-d).²⁹ To evaluate the feasibility of electron transfer events proposed in the reaction mechanism, DFT calculations using Gaussian software were conducted to examine the frontier molecular orbital energies (Scheme 4F). The HOMO energy of substrate **1a** was found to be significantly higher than the LUMO of EY, indicating a thermodynamically favorable single-electron transfer from **1a** to the EY*. Similarly, intermediate **II** also exhibits a HOMO energy level that lies above the LUMO energy level of EY, suggesting its potential to undergo a comparable SET process with EY*. These orbital energy relationships strongly support a photoinduced SET pathway and emphasize the function of eosin Y as

a competent electron acceptor in facilitating radical generation under visible light conditions.

Based on the above mechanistic studies, DFT calculations, and previous reports,^{30–32} we propose a working mechanistic hypothesis (Scheme 4G). The catalytic cycle is initiated by the photoexcitation of eosin Y (EY) under visible light, generating its strongly oxidizing excited state (EY*). This excited EY* undergoes a single-electron transfer with **1a**, forming a transient acyl radical **I** (trapped experimentally as TEMPO adduct **6a**) and the eosin Y radical anion (EY^{•-}). Acyl radical **I** then reacts irreversibly with styrene derivative **2a** to afford **II**, a process that is thermodynamically favorable with a driving force of 18.57 kcal mol⁻¹ (also supported by the formation of TEMPO adduct **7a**). Subsequently, a reductive quenching cycle involving EY facilitates the conversion of radical **II** to carbocation **III**, proceeding through an activation barrier of 114.64 kcal mol⁻¹. The photocatalytic cycle is completed by electron transfer from EY^{•-} to molecular oxygen, generating the superoxide anion radical (O₂^{•-}), which eventually forms hydrogen peroxide. Finally, a base abstracts a hydrogen atom from carbocation **III**, resulting in the formation of a double bond and yielding the desired product **3**.

Conclusion

In the final analysis, we developed a direct decarboxylative acylation of styrene with an oxo acid that is highly efficient and visible light-initiated, utilizing eosin Y to get an α,β -unsaturated ketone. The reaction conditions were well tolerated by the functional groups, and moderate to excellent yields of the necessary α,β -unsaturated ketones were obtained. Because chalcone derivatives have the ketoethylenic moiety –CO–CH=CH–, they are regarded as desirable species. The reactive α,β -unsaturated carbonyl group of chalcones and their derivatives gives them an extensive variety of pharmacological activities, notably antiproliferative, antifungal, antibacterial, antiviral, antileishmanial, and antimalarial activities. With these benefits, this novel methodology will broaden the range of synthetic methods for various chalcones in the industrial and medicinal domains while also satisfying the requirements of green and sustainable chemistry.

Author contributions

The project was created and designed by Aman Singh and Ambuj Kumar Kushwaha. The synthesis, tests, and characterisation studies were carried out by Aman Singh. Some substrates were synthesized by Ankur Yadav. Sundaram Singh, Pooja Kumari, and Shikha Pandey discussed about the experimental conclusions. The manuscript was written by Aman Singh. The manuscript was revised by Sundaram Singh and Ambuj Kumar Kushwaha.

Conflicts of interest

There aren't any conflicts of interest.



Data availability

CCDC 2470266 contains the supplementary crystallographic data for this paper.³³

The data supporting this article have been included as part of the supplementary information (SI) (general information, experimental details, mechanistic study data for products, and NMR and mass spectra of products). Supplementary information is available. See DOI: <https://doi.org/10.1039/d5su00684h>.

Acknowledgements

The authors are thankful for the instrumentation facilities provided by CIFIC, IIT (BHU) and the financial support provided by the CSIR (JRF) (Aman Singh) and SERB project (CRG/2023/008284).

References

- M. H. Shaw, J. Twilton and D. W. C. MacMillan, *J. Org. Chem.*, 2016, **81**, 6898–6926.
- A. K. Kushwaha, S. K. Maury, S. Kumari, A. Kamal, H. K. Singh, D. Kumar and S. Singh, *Synthesis*, 2022, **54**, 5099–5109.
- S. B. Beil, T. Q. Chen, N. E. Intermaggio and D. W. C. MacMillan, *Acc. Chem. Res.*, 2022, **55**, 3481–3494.
- A. Noble, S. J. McCarver and D. W. C. MacMillan, *J. Am. Chem. Soc.*, 2015, **137**, 624–627.
- W.-F. Tian, C.-H. Hu, K.-H. He, X.-Y. He and Y. Li, *Org. Lett.*, 2019, **21**, 6930–6935.
- A. Rahaman, S. S. Chauhan and S. Bhadra, *Org. Biomol. Chem.*, 2023, **21**, 5691–5724.
- S. Lu, Y. Xiang, J. Chen and C. Shu, *Molecules*, 2024, **29**, 3904.
- G.-Z. Wang, R. Shang, W.-M. Cheng and Y. Fu, *Org. Lett.*, 2015, **17**, 4830–4833.
- F. Penteado, E. F. Lopes, D. Alves, G. Perin, R. G. Jacob and E. J. Lenardão, *Chem. Rev.*, 2019, **119**, 7113–7278.
- A. K. Kushwaha, A. Kamal, H. K. Singh, S. K. Maury, T. Mondal and S. Singh, *Org. Lett.*, 2024, **26**, 1416–1420.
- B. Salehi, C. Quispe, I. Chamkhi, N. El Omari, A. Balahbib, J. Sharifi-Rad, A. Bouyahya, M. Akram, M. Iqbal, A. O. Docea, C. Caruntu, G. Leyva-Gómez, A. Dey, M. Martorell, D. Calina, V. López and F. Les, *Front. Pharmacol.*, 2021, **11**, 592654.
- N. A. A. Elkanzi, H. Hrichi, R. A. Alolayan, W. Derafa, F. M. Zahou and R. B. Bakr, *ACS Omega*, 2022, **7**, 27769–27786.
- K. Mezgebe, Y. Melaku and E. Mulugeta, *ACS Omega*, 2023, **8**, 19194–19211.
- Q. Jiang, J. Jia, B. Xu, A. Zhao and C.-C. Guo, *J. Org. Chem.*, 2015, **80**, 3586–3596.
- S. Wu, H. Yu, Q. Hu, Q. Yang, S. Xu and T. Liu, *Tetrahedron Lett.*, 2017, **58**, 4763–4765.
- M. Zhang, J. Xi, R. Ruzi, N. Li, Z. Wu, W. Li and C. Zhu, *J. Org. Chem.*, 2017, **82**, 9305–9311.
- A. M. Davies, R. D. Hernandez and J. A. Tunge, *Chem.–Eur. J.*, 2022, **28**, e202202781.
- S. Mondal, S. P. Midya, S. Mondal, S. Das and P. Ghosh, *Chem.–Eur. J.*, 2024, **30**, e202303337.
- S. Pandey, A. Kamal, A. K. Kushwaha, H. K. Singh, S. K. Maury and S. Singh, *Chem. Commun.*, 2024, **60**, 1136–1139.
- S. Pandey, A. Kamal, A. Kumar Kushwaha and S. Singh, *Asian J. Org. Chem.*, 2025, **14**, e202400409.
- A. Kamal, H. K. Singh, S. K. Maury, A. K. Kushwaha, V. Srivastava and S. Singh, *Asian J. Org. Chem.*, 2023, **12**, e202200632.
- A. K. Kushwaha, S. K. Maury, A. Kamal, H. K. Singh, S. Pandey and S. Singh, *Chem. Commun.*, 2023, **59**, 4075–4078.
- S. Pandey, S. Kumar, V. Singh, V. Srivastava and S. Singh, *J. Org. Chem.*, 2025, **90**(19), 6423–6433.
- S. Pandey, A. Singh, A. K. Kushwaha and S. Singh, *J. Org. Chem.*, 2024, **89**, 12576–12582.
- A. K. Kushwaha, A. Kamal, P. Kumari and S. Singh, *Org. Lett.*, 2024, **26**, 3796–3800.
- M. H. Shaw, J. Twilton and D. W. C. MacMillan, *J. Org. Chem.*, 2016, **81**, 6898–6926.
- N. Jubair, M. Rajagopal, S. Chinnappan, N. B. Abdullah and A. Fatima, *Evid. base Compl. Alternative Med.*, 2021, **2021**, 3663315.
- S. Tekale, S. Mashele, O. Poee, S. Thore, P. Kendrekar, R. Pawar, S. Tekale, S. Mashele, O. Poee, S. Thore, P. Kendrekar and R. Pawar, in *Vector-Borne Diseases – Recent Developments in Epidemiology and Control*, IntechOpen, 2020.
- S. B. Gavanaroudi, *Eurasian J. Chem. Med. Pet. Res.*, 2024, **3**, 18–32.
- J. Tripathi, H. Gupta and A. Sharma, *Org. Lett.*, 2025, **27**, 1018–1023.
- A. Tlahuext-Aca, R. A. Garza-Sanchez, M. Schäfer and F. Glorius, *Org. Lett.*, 2018, **20**, 1546–1549.
- C. Zhou, P. Li, X. Zhu and L. Wang, *Org. Lett.*, 2015, **17**, 6198–6201.
- CCDC 2470266: Experimental Crystal Structure Determination, 2025, DOI: [10.5517/ccdc.csd.cc2nxj04](https://doi.org/10.5517/ccdc.csd.cc2nxj04).

